

Orbital-selective Mott transition in multiband systems: Slave-spin representation and dynamical mean-field theory

L. de'Medici,^{1,2} A. Georges,¹ and S. Biermann¹¹*Centre de Physique Théorique, École Polytechnique 91128 Palaiseau Cedex, France*²*Laboratoire de Physique des Solides, CNRS-UMR 8502, Université de Paris-Sud, Bâtiment 510, 91405 Orsay, France*

(Received 1 April 2005; revised manuscript received 8 August 2005; published 22 November 2005)

We examine whether the Mott transition of a half-filled, two-orbital Hubbard model with unequal bandwidths occurs simultaneously for both bands or whether it is a two-stage process in which the orbital with narrower bandwidth localizes first (giving rise to an intermediate “orbital-selective” Mott phase). This question is addressed using both dynamical mean-field theory and a representation of fermion operators in terms of slave quantum spins, followed by a mean-field approximation (similar in spirit to a Gutzwiller approximation). In the latter approach, the Mott transition is found to be orbital selective for all values of the Coulomb exchange (Hund) coupling J when the bandwidth ratio is small and only beyond a critical value of J when the bandwidth ratio is larger. Dynamical mean-field theory partially confirms these findings, but the intermediate phase at $J=0$ is found to differ from a conventional Mott insulator, with spectral weight extending down to arbitrary low energy. Finally, the orbital-selective Mott phase is found, at zero temperature, to be unstable with respect to an interorbital hybridization V and replaced at small V by a state with a large effective mass (and a low quasiparticle coherence scale) for the narrower band.

DOI: [10.1103/PhysRevB.72.205124](https://doi.org/10.1103/PhysRevB.72.205124)

PACS number(s): 71.30.+h, 71.10.Fd, 71.27.+a

I. INTRODUCTION

The Mott metal-insulator transition plays a central role in the physics of all strongly correlated electron materials. At a qualitative level, localization of the electrons can occur when the kinetic energy gain (typically given by the bare bandwidth) is smaller than the cost in on-site repulsive Coulomb energy (U). In recent years, dynamical mean-field theory¹⁻³ (DMFT) has provided a consistent theoretical framework which has advanced our understanding of this phenomenon,^{1,4} in particular through the study of simplified models such as the one-band Hubbard model.

In real materials, however, such as transition-metal oxides, several orbital components are involved. Crystal-field effects and the Coulomb exchange energy (J) affect the energy of on-site atomic states, which no longer depend only on the total local charge as in the orbitally degenerate case. Furthermore, the intersite hopping amplitudes can be significantly different for different orbital components (due, e.g., to their relative orientations). It is therefore essential to understand how these effects can affect the Mott transition and whether qualitatively new effects are possible when the orbital degeneracy is lifted.

Recently, this question has attracted a lot of attention. In their study of $\text{Ca}_{2-x}\text{Sr}_x\text{RuO}_4$, Anisimov *et al.*⁵ suggested that a partial localization could take place, in which some orbital components (with broader bandwidth) are conducting, while others (with narrower bandwidth) are localized (see also Ref. 6). Following this proposal, several studies have been performed in the model context, with controversial results.⁷⁻¹¹ Liebsch^{7,10} initially challenged the existence of such an “orbital-selective Mott transition” (OSMT) on the basis of DMFT calculations. Koga and co-workers,^{9,11} on the other hand, did find an OSMT within their DMFT calculations and suggested that a unique transition is found only if $J=0$. A

symmetry argument was put forward to explain this finding.

In this paper, a clarification of this problem is attempted, using DMFT and another, complementary approach. The latter is based on a representation of fermion operators in terms of slave quantum spins, specifically forged to address multiorbital models (Sec. III). A mean-field approximation based on this representation, similar in spirit to the Gutzwiller approximation, provides a fast and efficient method in order to investigate the Mott transition in a wide range of parameters (Sec. IV). In Sec. V, a detailed study of the previously unexplored regime in which one of the bands is much narrower than the other and $J=0$ is presented, using exact diagonalizations and quantum Monte Carlo methods in the DMFT framework. Finally (Sec. VI), the effect of an interband hybridization is considered.

II. MODEL

The model considered in this paper is a tight-binding model for two bands coupled by local interactions. The Hamiltonian reads $H=H_0+H_{int}$, where H_0 is the noninteracting part:

$$H_0 = - \sum_{m=1,2} t_m \sum_{\langle ij \rangle, \sigma} d_{im\sigma}^\dagger d_{jm\sigma} + \text{H.c.} + \sum_{i,m\sigma} (\epsilon_m - \mu) d_{im\sigma}^\dagger d_{im\sigma}, \quad (1)$$

in which $d_{im\sigma}^\dagger$ ($d_{im\sigma}$) creates (annihilates) an electron on the site i , in the orbital m , with spin σ . The ϵ_m 's are crystal-field levels, and μ is the chemical potential, kept here for generality. In most of the paper, however, we shall focus on the case of the zero crystal-field splitting ($\epsilon_1=\epsilon_2=0$) and half-filling of each band (i.e., one electron per site in each orbital, which corresponds to $\mu=0$ given our normalization of the interaction term). At the end of the paper, we shall also con-

sider the possibility of a nonzero interorbital hybridization.

The full interaction, in the case of degenerate bands in a cubic environment,^{12,13} reads

$$H_{int} = U \sum_{im} \tilde{n}_{im\uparrow} \tilde{n}_{im\downarrow} + U' \sum_{i\sigma} \tilde{n}_{i1\sigma} \tilde{n}_{i2\bar{\sigma}} + (U' - J) \sum_{i\sigma} \tilde{n}_{i1\sigma} \tilde{n}_{i2\sigma} - J \sum_i [d_{i1\uparrow}^\dagger d_{i1\downarrow} d_{i2\downarrow}^\dagger d_{i2\uparrow} + d_{i1\downarrow}^\dagger d_{i1\uparrow} d_{i2\uparrow}^\dagger d_{i2\downarrow}] - J \sum_i [d_{i1\uparrow}^\dagger d_{i1\downarrow} d_{i2\uparrow}^\dagger d_{i2\downarrow} + d_{i2\uparrow}^\dagger d_{i2\downarrow} d_{i1\uparrow}^\dagger d_{i1\downarrow}], \quad (2)$$

where $\tilde{n}_{im\sigma} \equiv n_{im\sigma} - 1/2$. Following Castellani *et al.*,¹² the reduction of the Coulomb interorbital Coulomb interactions U' as compared to the interorbital U is related to the Hund's coupling J by

$$U' = U - 2J. \quad (3)$$

In the case of vanishing Hund's rule coupling $J=0$ the interaction vertex $[=U(n_1+n_2-2)^2/2]$ thus depends only on the total charge, while if $J \neq 0$, the interorbital interaction is weaker than the intraorbital one and becomes sensitive to the spin configuration.

III. SLAVE-SPIN MEAN-FIELD THEORY

A. Slave-spin representation

In this section, we introduce a new representation of fermion operators in terms of constrained ("slave") auxiliary fields, which proves to be particularly convenient in order to study the multiorbital Hamiltonian above. The main idea at the root of any slave-variable representation is to enlarge the Hilbert space and to impose a local constraint in order to eliminate the unphysical states. When the constraint is treated on average, a mean-field approximation is obtained. Different slave-field representations will lead to different mean-field theories. The quality of the mean-field approximation can be improved by tailoring the choice of slave fields to the specific problem under consideration. In general, a compromise has to be found between the simplicity of the representation, the number of unphysical states which are introduced, and the possibility of an analytical treatment of the resulting mean-field theory.

For finite- U Hubbard models, Kotliar and Ruckenstein¹⁴ have introduced a slave-boson representation which can be used in the present context, when appropriately generalized to multiorbital models (in the spirit of the Gutzwiller approximation¹⁵). However, this method introduces many variational parameters. On the opposite, Florens and Georges introduced a very economical representation of the N -orbital Hubbard model with $SU(N)$ symmetry based on a single slave variable, taken to be the phase conjugate to the total charge on a given lattice site (slave-rotor representation).^{16,17} However, this method is not appropriate when the orbital symmetry is broken, as in the present work.

Here, we introduce a new slave-variable representation³⁰ especially suited for dealing with multiband models and addressing orbital-dependent properties. The basic observation behind this scheme is that the two possible occupancies of a

spinless fermion on a given site, $n_d=0$ and $n_d=1$, can be viewed as the two possible states of a spin-1/2 variable, $S^z = -1/2$ and $S^z = +1/2$. This representation has been widely used in the case of hard-core bosons. In the fermionic context, however, one needs to ensure anticommutation properties, and this is done by introducing an auxiliary fermion f , with the additional local constraint

$$f^\dagger f = S^z + \frac{1}{2}. \quad (4)$$

In this manner, one obtains a faithful representation of the Hilbert space, which reads

$$|0\rangle = |n_f = 0, S^z = -1/2\rangle, \quad (5)$$

$$|1\rangle \equiv d^\dagger |0\rangle = |n_f = 1, S^z = +1/2\rangle. \quad (6)$$

This constraint eliminates the two unphysical states $|n_f = 0, S^z = +1/2\rangle$ and $|n_f = 1, S^z = -1/2\rangle$. This representation is easily extended to the multiorbital case by treating each orbital and spin species in this manner. Hence a set of $2N$ spin-1/2 variables $S_{m\sigma}^z$ and auxiliary fermions $f_{m\sigma}$ is introduced ($m=1, \dots, N$ is the number of orbitals), obeying the local constraint on each site:

$$\hat{n}_{im\sigma}^f = S_{im\sigma}^z + \frac{1}{2}. \quad (7)$$

This constraint can, e.g., be imposed with Lagrange multiplier fields $\lambda_{im\sigma}(\tau)$.

We now explain how to rewrite the original Hamiltonian (1) and (2) in terms of the slave spins and auxiliary fermions. We consider first for simplicity the case $J=0$, since the case $J \neq 0$ requires an additional approximation, as discussed later. For $J=0$, the interaction involves only the total electron charge on a given site and therefore reads

$$H_{int}^{J=0} \equiv \frac{U}{2} \sum_i \left(\sum_{m,\sigma} \tilde{n}_{im\sigma} \right)^2 = \frac{U}{2} \sum_i \left(\sum_{m,\sigma} S_{im\sigma}^z \right)^2. \quad (8)$$

In order to express the noninteracting part of the Hamiltonian, we need to choose an appropriate representation of the creation operator of a physical electron, $d_{im\sigma}^\dagger$. There is some freedom associated with this, since different operators in the enlarged Hilbert space spanned by the slave-spin and auxiliary fermions can have the same action on the physical (constrained) Hilbert space. We have not used the obvious possibility $d^\dagger \rightarrow S^+ f^\dagger$, $d \rightarrow S^- f$. This representation is correct in the physical Hilbert space (i.e., when the constraint is treated exactly), but it can be shown that additional mean-field approximations based on this representation will ultimately lead to a problem with spectral weight conservation because S^+ and S^- do not commute. Instead, we have chosen the representation $d^\dagger \rightarrow 2S^x f^\dagger$, $d \rightarrow 2S^x f$, which is identical to the previous one on the physical Hilbert space and involves commuting slave-spin operators. With this choice, the noninteracting part of the Hamiltonian reads

$$H_0 = - \sum_m t_m \sum_{\langle ij \rangle, \sigma} 4S_{im\sigma}^x S_{jm\sigma}^x (f_{im\sigma}^\dagger f_{jm\sigma} + \text{H.c.}) \\ + \sum_{i,m\sigma} (\epsilon_m - \mu) f_{im\sigma}^\dagger f_{im\sigma}.$$

At this stage, no approximation has been made, provided the constraint is treated exactly.

B. Mean-field approximation

Approximations will now be introduced, which consists of three main steps: (i) treating the constraint on average, using a static and site-independent Lagrange multiplier $\lambda_{m\sigma}$, (ii) decoupling the auxiliary fermions and slave-spin degrees of freedom, and finally (iii) treating the slave-spin Hamiltonian in a single-site mean-field approach. This last step is quite independent of the two previous ones and can be rather easily improved on, as done in Ref. 17.

After the first two steps, one obtains two effective Hamiltonians

$$H_{eff}^f = - \sum_m t_m^{eff} \sum_{\langle ij \rangle, \sigma} (f_{im\sigma}^\dagger f_{jm\sigma} + \text{H.c.}) \\ + \sum_{i,m\sigma} (\epsilon_m - \mu - \lambda_m) f_{im\sigma}^\dagger f_{im\sigma}, \quad (9)$$

$$H_{eff}^S = - \sum_m 4J_m^{eff} \sum_{\langle ij \rangle, \sigma} S_{im\sigma}^x S_{jm\sigma}^x + \sum_{i,m\sigma} \lambda_m \left(S_{im\sigma}^z + \frac{1}{2} \right) \\ + H_{int}[\{\vec{S}_{im\sigma}\}], \quad (10)$$

with $H_{int}[\{\vec{S}_{im\sigma}\}] = U/2 \sum_i (\sum_{m\sigma} S_{im\sigma}^z)^2$ for $J=0$. In these expressions, t_m^{eff} and J_m^{eff} are effective hoppings and slave-spin exchange constants which are determined from the self-consistency equations

$$t_m^{eff} = 4t_m \langle S_{im\sigma}^x S_{jm\sigma}^x \rangle, \quad (11)$$

$$J_m^{eff} = t_m \langle f_{im\sigma}^\dagger f_{jm\sigma} + f_{jm\sigma}^\dagger f_{im\sigma} \rangle. \quad (12)$$

The free-fermion Hamiltonian (9) describes the quasiparticle degrees of freedom. Their effective mass is set by the renormalization of the hopping: $t_m^{eff}/t_m = 4 \langle S_{im\sigma}^x S_{jm\sigma}^x \rangle$. The quasiparticle weight is associated with a different quantity: namely,

$$Z_m = 4 \langle S_{im\sigma}^x \rangle^2. \quad (13)$$

Note that it depends in general on the orbital, a key feature for the physics that we want to address with this technique. Both the renormalization of the mass and the quasiparticle weight are self-consistently determined from the solution of the quantum-spin Hamiltonian (10), which describes the charge dynamics. As is clear from Eq. (13), metallic behavior for orbital m corresponds to long-range order in S_m^x , while Mott insulating behavior corresponds to $\langle S_m^x \rangle = 0$.

At this stage, the slave-spin degrees of freedom are still described by a quantum-spin Hamiltonian on the lattice, and we therefore make the additional approximation (iii) of treating this model on the level of a single-site mean field. We

thus have to solve the single-site spin Hamiltonian

$$H_s = \sum_{m\sigma} 2h_m S_{m\sigma}^x + \sum_{m\sigma} \lambda_m \left(S_{m\sigma}^z + \frac{1}{2} \right) + H_{int}[\vec{S}_{m\sigma}], \quad (14)$$

in which the mean field h_m is determined self-consistently from

$$h_m = 2z J_m^{eff} \langle S_{m\sigma}^x \rangle, \quad (15)$$

where z is the coordination number of the lattice. This equation can be combined with Eq. (12) to yield

$$h_m = 4 \langle S_{m\sigma}^x \rangle \frac{1}{\mathcal{N}} \sum_{\mathbf{k}} \epsilon_{\mathbf{k}m} \langle f_{\mathbf{k}m\sigma}^\dagger f_{\mathbf{k}m\sigma} \rangle. \quad (16)$$

In this expression, the fermionic expectation value is to be calculated with the quasiparticle Hamiltonian (9). Within this single-site mean-field approximation, however, the renormalization of the hopping becomes identical to the quasiparticle residue since $\langle S_{im\sigma}^x S_{jm\sigma}^x \rangle$ factorizes into $\langle S_{im\sigma}^x \rangle^2$. As a result, the quasiparticle Hamiltonian reads

$$H_{eff}^f = \sum_{\mathbf{k}, m\sigma} (Z_m \epsilon_{\mathbf{k}m} + \epsilon_m - \mu - \lambda_m) f_{\mathbf{k}m\sigma}^\dagger f_{\mathbf{k}m\sigma}, \quad (17)$$

with $\epsilon_{\mathbf{k}m} \equiv -t_m / z \sum_{j,n,n(i)} e^{-\mathbf{k} \cdot (\mathbf{i}-\mathbf{j})}$ the Fourier transform of the hopping. Equations (13), (14), (16), and (17) and the constraint equation (7) self-consistently determine the variational parameters h_m , λ_m , and $Z_m = 4 \langle S_{m\sigma}^x \rangle^2$. They are the basic mean-field equations based on the slave-spin representation, which will be used below. Solving these equations requires one to diagonalize the single-site spin Hamiltonian (14), corresponding to a $4^N \times 4^N$ matrix.

Let us finally discuss the case of a nonzero Hund's coupling $J \neq 0$. The first three terms in Eq. (2) are easy to treat in the slave-spin formalism, since they involve only density-density interactions and are thus directly expressed in terms of the Ising components of the slave spins. They read

$$\frac{U'}{2} \sum_i \left(\sum_{m,\sigma} S_{im\sigma}^z \right)^2 + J \sum_{i,m} \left(\sum_{\sigma} S_{im\sigma}^z \right)^2 - \frac{J}{2} \sum_{i,\sigma} \left(\sum_m S_{im\sigma}^z \right)^2. \quad (18)$$

In contrast, the ‘‘spin-flip’’ and (intrasite) ‘‘pair-hopping’’ terms [last two terms in Eq. (2)] are more difficult to deal with, since they involve both slave-spin and auxiliary fermions operators. As a result, four-fermion terms are introduced which require additional mean-field decouplings. For simplicity, we choose to mimic the effect of these terms by replacing them by operators which have exactly the same effect on the slave-spin quantum numbers of the Hilbert space: namely,

$$-J \sum_i [S_{i1\uparrow}^+ S_{i1\downarrow}^- S_{i2\downarrow}^+ S_{i2\uparrow}^- + S_{i1\downarrow}^+ S_{i1\uparrow}^- S_{i2\uparrow}^+ S_{i2\downarrow}^-] \\ -J \sum_i [S_{i1\uparrow}^+ S_{i1\downarrow}^+ S_{i2\uparrow}^- S_{i2\downarrow}^- + S_{i2\uparrow}^+ S_{i2\downarrow}^- S_{i1\uparrow}^- S_{i1\downarrow}^-], \quad (19)$$

Despite the fact that these terms connect the physical and unphysical parts of the Hilbert space (and therefore would strictly vanish if the constraint was implemented exactly), it

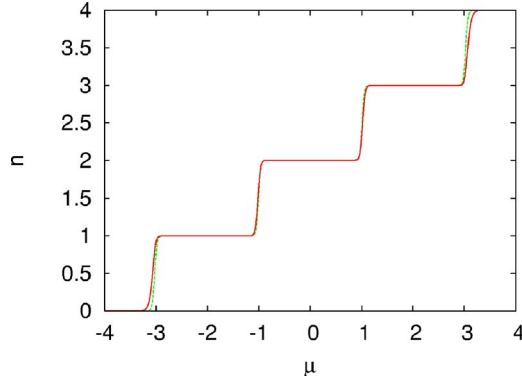


FIG. 1. (Color online) Filling vs chemical potential for a two-orbital impurity (atomic limit of a particle-hole-symmetric Hubbard model), $U=2$, $\beta=50$: within the slave-spin mean-field (solid line) and exact (dashed line) results. The Coulomb staircase is correctly reproduced up to temperatures of order $\sim U$.

is reasonable to expect that they will qualitatively describe the physics of the spin-flip and pair-hopping terms when the constraint is treated on average, because their action on the slave-spin quantum numbers is the correct one. Hence, we shall use the following representation of the interacting part of the Hamiltonian for $J \neq 0$:

$$\begin{aligned}
 H_{int} \approx & \frac{U'}{2} \sum_i \left(\sum_{m,\sigma} S_{im\sigma}^z \right)^2 + J \sum_{i,m} \left(\sum_{\sigma} S_{im\sigma}^z \right)^2 - \frac{J}{2} \sum_{i,\sigma} \left(\sum_m S_{im\sigma}^z \right)^2 \\
 & - J \sum_i [S_{i1\uparrow}^+ S_{i1\downarrow}^- S_{i2\downarrow}^+ S_{i2\uparrow}^- + S_{i1\downarrow}^+ S_{i1\uparrow}^- S_{i2\uparrow}^+ S_{i2\downarrow}^-] \\
 & - J \sum_i [S_{i1\uparrow}^+ S_{i1\downarrow}^+ S_{i2\uparrow}^- S_{i2\downarrow}^- + S_{i2\uparrow}^+ S_{i2\downarrow}^+ S_{i1\uparrow}^- S_{i1\downarrow}^-]. \quad (20)
 \end{aligned}$$

C. Benchmarks

In this section, we perform some benchmarks of the slave-spin representation and mean-field theory.

1. Atomic limit ($J=0$)

In the $J=0$ case we check explicitly that the atomic limit (i.e., $t_m=0$) of the degenerate N -band model with $SU(2N)$ symmetry is correctly reproduced. Indeed our equations simplify drastically in this limit ($\tilde{t}_m=h_m=0$), leaving only the $\lambda_{m\sigma}=\bar{\lambda}$ to be determined. The constraint equation (7) reads, in this case,

$$n_F(\mu - \bar{\lambda}) = \mathcal{Z}^{-1} \sum_{Q=0}^{2N} \mathcal{N}_Q Q e^{-\beta[(U/2)(Q-N)^2 + \bar{\lambda}Q]}, \quad (21)$$

where $n_F(\epsilon)$ is the Fermi function, $\mathcal{Z} \equiv \sum_{Q=0}^{2N} \mathcal{N}_Q \exp[-\beta[(U/2)(Q-N)^2 + \bar{\lambda}Q]]$, $\mathcal{N}_Q \equiv \binom{2N}{Q}$, and Q is the total number of particles. Solving numerically this equation for $\bar{\lambda}$ leads to the correct ‘‘Coulomb staircase,’’ as shown in Fig. 1, as long as $T \ll U$. At high temperatures the fact that we have imposed the constraints only in average limits the accuracy, but in practice $T \ll U$ is not a severe limitation.

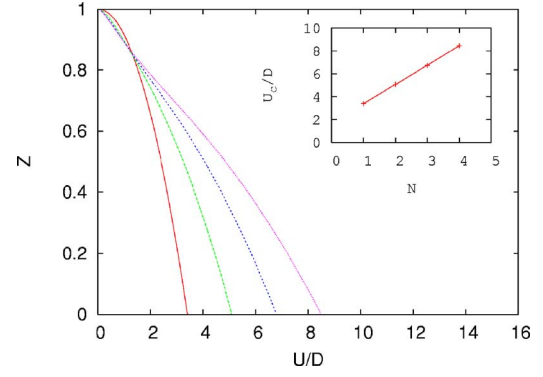


FIG. 2. (Color online) Quasiparticle weight, obtained from slave-spin mean-field theory, for the N -orbital Hubbard model at half-filling (with, from left to right, $N=1, 2, 3, 4$). The noninteracting density of states is a semicircle with half-bandwidth D . Inset: Dependence of the critical U on N . The exact large- N behavior is obtained.

2. N -orbital Hubbard model with $SU(2N)$ symmetry and large- N limit

Here, we apply the slave-spin mean-field approximation to the N -orbital model ($m=1, \dots, N$), in the case where all bands have the same hopping, with $J=0$. The results for the quasiparticle weight as a function of U , at half-filling, are displayed in Fig. 2. A transition into a Mott phase is found for $U > U_c(N)$. The exact large- N behavior of $U_c(N)$ in the limit of infinite coordination (DMFT) is known¹⁸ to be linear in N , the slope being $U_c/N=8|\bar{\epsilon}|$, where $\bar{\epsilon} \equiv \int_{-\infty}^0 d\epsilon D(\epsilon)\epsilon$. This slope is correctly reproduced by the slave-spin mean-field approximation, indicating that this approximation becomes more accurate as N is increased.

One can actually calculate analytically the critical value of the coupling within this approach, for arbitrary N , by performing a perturbative expansion around the atomic limit for small h_m . This yields

$$U_c = 8(N+1)|\bar{\epsilon}|, \quad (22)$$

which coincides with the numerical determination in the inset of Fig. 2. We also note that Eq. (22) is precisely the result of the Gutzwiller (slave-boson) approximation in the multi-orbital case.

D. Comparison with slave bosons and slave rotors

As suggested by the fact they yield identical values of U_c , the slave-spin mean-field theory has many similarities with the Gutzwiller approximation (GA). In fact, as shown in Fig. 3, in the one-band Hubbard model the whole dependence of Z on U is identical to that of the GA.

The slave-spin representation has several advantages over the slave-boson representations that can be used to formulate the GA. One advantage is that the number of variables is smaller: $2N$ spin-1/2 degrees of freedoms instead of 2^N slave bosons (one associated with each state in the Hilbert space, in the absence of symmetries). Another advantage is that the number of unphysical states is smaller than in slave-boson representations, because the Hilbert space spanned by the $2N$

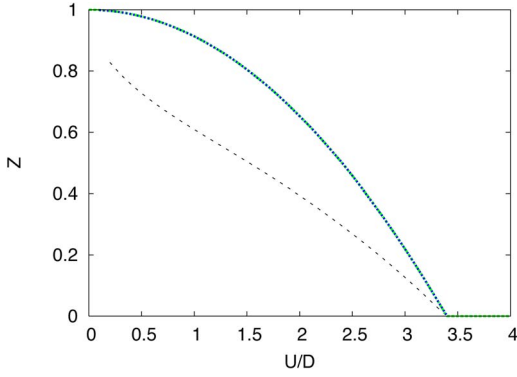


FIG. 3. (Color online) Quasiparticle weight of the one-band Hubbard model, obtained with slave rotors (thin line), slave spins, and the Gutzwiller (slave-boson) approximations (thick lines). The latter two actually coincide. The small- U behavior of the slave-rotor approach is due to the larger number of unphysical states (see text).

quantum spins is finite by construction, while the Hilbert space associated with the slave bosons in the absence of the constraint is an infinite-dimensional one. This might be useful in considering finite-temperature properties and the entropy of the model.

A similar remark applies when comparing the present slave-spin representation to the slave-rotor representation recently developed by Florens and Georges.^{16,17} This representation is specifically tailored to $SU(2N)$ -symmetric models and is very economical since it introduces only *one* slave variable. Specifically, a (slave) quantum rotor and auxiliary fermions are introduced on each site such that

$$d_{im\sigma}^\dagger = f_{im\sigma}^\dagger e^{i\theta_i}, \quad d_{im\sigma} = f_{im\sigma} e^{-i\theta_i}, \quad (23)$$

where the phase is conjugate to the local charge, corresponding to the local constraint

$$\sum_{m\sigma} \left(f_{im\sigma}^\dagger f_{im\sigma} - \frac{1}{2} \right) = \hat{L}_i, \quad (24)$$

in which $\hat{L}_i = 1/i\partial/\partial\theta_i$ is the conjugate momentum to the phase. It is clear from these expressions that there is a close similarity between the slave-spin and slave-rotor formalisms. Two important differences must be noted: (i) a single slave-rotor variable is introduced for all orbitals and (ii) the Hilbert space of the unconstrained rotor is infinite dimensional, containing an infinite tower of charge states $|l\rangle$ which are physical only for $|l| \leq N$. As a result, mean-field approximations in which the constraint is treated only on average are less accurate when the contribution of these unphysical charge states become sizable. This is particularly true in the weak-coupling limit. In Fig. 3, we compare the slave-spin and slave-rotor result for the quasiparticle residue in the one-band case, in order to illustrate this effect.

On the whole, slave rotors and slave spins offer two useful representations, the former being very economical and well suited to situations in which only the total local charge is involved (e.g., in Coulomb blockade problems¹⁹), while the latter is well suited to the investigation of orbital-dependent properties, as in the present article. Both methods

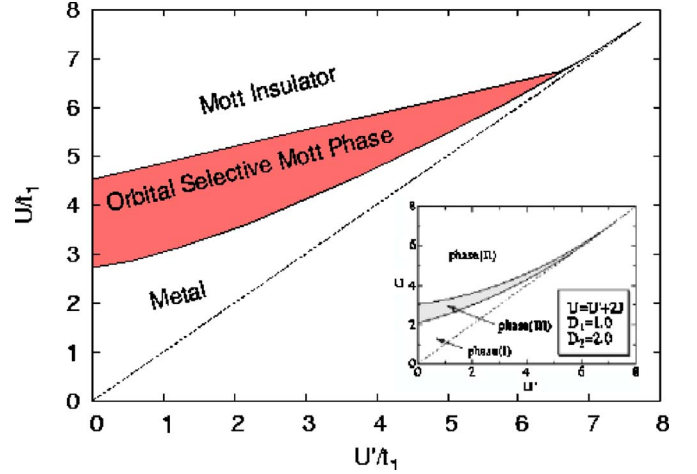


FIG. 4. (Color online) Phase diagram (U vs U') for $t_2/t_1=0.5$ at $T=0$ within the slave-spin mean-field theory. Inset: same diagram obtained with exact diagonalization dynamical mean-field theory (ED-DMFT) in Ref. 9. The dotted line indicates $J=0$ —i.e., $U=U'$. In “phase I” both bands are metallic; in “phase II” both bands are insulating. “Phase III” is the orbital-selective Mott phase.

are easy to implement at a very low numerical cost, hence allowing for a fast and efficient investigation of the phase diagram and phase transitions in a wide range of parameters.

IV. ORBITAL-SELECTIVE MOTT TRANSITION WITH SLAVE-SPIN MEAN-FIELD THEORY

In this section, we use slave-spin mean-field theory in order to study the two-band model with unequal hoppings. The noninteracting density of states of each band is taken to be a semicircle (of half-width $D_1=2t_1$ and $D_2=2t_2 < D_1$), corresponding to a Bethe lattice with infinite connectivity $z = \infty$ and nearest-neighbour hoppings $t_{1,2}/\sqrt{z}$. No crystal-field splitting is introduced ($\epsilon_1 = \epsilon_2 = 0$), and we restrict ourselves to the case in which both bands are half-filled ($\langle n_1 \rangle = \langle n_2 \rangle = 1$). The model is thus particle-hole symmetric, implying that the chemical potential $\mu=0$ and Lagrange multipliers $\lambda_1 = \lambda_2 = 0$. The parameter space was explored for $U > 0$, $J = 0$ to $0.5U$ (i.e., $U' = U - 2J = 0$ to U) and the ratio between the two bandwidths, $t_2/t_1 = 0-1.0$. For the study of the Mott transitions in this model we monitor the quasiparticle weights $Z_m = 4\langle S_{m\sigma}^x \rangle^2$.

Figure 4 displays the phase diagram within slave-spin mean-field theory for the bandwidth ratio $t_2/t_1=0.5$. Three different phases are found: at small U both bands are metallic (i.e., $Z_m \neq 0$), at large U both are insulating ($Z_m = 0$), and in between an OSMP is found in which only the band with largest bandwidth has $Z_1 \neq 0$, while the narrower band has $Z_2 = 0$.

In the inset of Fig. 4, we reproduce for comparison the result of Koga *et al.*⁹ obtained within DMFT. Qualitatively, one sees that the slave-spin mean field compares rather well to the DMFT results. There are quantitative differences in the critical values of the couplings U and U' , a well-known feature of Gutzwiller-like approximations. Also, the linear de-

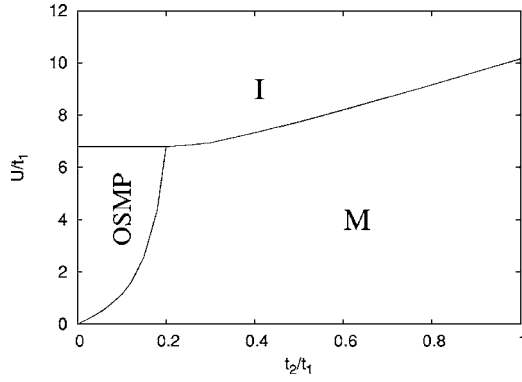


FIG. 5. Dependence of the critical U on the ratio t_2/t_1 at $J=0$ and $T=0$. All transitions are second order.

pendence on U' of the upper boundary of the OSMP phase is due to the simplified treatment of the spin-flip and pair-hopping terms discussed above (as indeed confirmed by the results of Sec. IV C).

There is, however, one significant qualitative difference between the slave-spin results and those of Koga *et al.* (inset). We find that the end point of the OSMP phase *does not lie exactly* on the $U=U'$ line. Hence, within the slave-spin mean field, the Mott transition becomes orbital selective (OSMT) only when J exceeds a critical value. This is a rather significant finding, since for $J=0$ the interacting part of the Hamiltonian (H_{int}) has full $SU(4)$ spin-orbital symmetry, while for $J \neq 0$ the symmetry is lower. In Ref. 9, it was argued that indeed the enhanced symmetry of the $J=0$ case prevents an orbital-selective Mott transition from occurring. Our finding that a critical value of J is needed to induce an OSMT (for $t_2/t_1=0.5$) suggests that symmetry considerations on H_{int} may not be essential to the existence of an orbital-selective transition. After all, the difference in bandwidths breaks the $SU(4)$ symmetry from the kinetic energy part of the Hamiltonian. In order to study this issue in more detail, we perform in the next section a detailed study of the $J=0$ case.

A. OSMT at $J=0$

In this section, we focus on the $J=0$ case, for which H_{int} has full $SU(4)$ symmetry, and explore the nature of the Mott transition in the full range of bandwidth ratio from $t_2/t_1=0$ to $t_2/t_1=1$.

We find that the two bands undergo a common Mott transition at a single value of $U=U_c$ as long as the bandwidth ratio exceeds a critical threshold: $t_2/t_1 > 0.2$. In contrast, for $t_2/t_1 < 0.2$, an *orbital-selective Mott phase is found*, despite the enhanced symmetry of the interaction term. Figure 5 displays our result for the phase diagram as a function of t_2/t_1 and U/t_1 . All transitions are found to be second order when $J=0$. In Fig. 6, the quasiparticle weights of each band are plotted as a function of U for several values of t_2/t_1 . The localization of the narrower band manifests itself as a kink in the quasiparticle weight of the wider band. As U is increased further, the wide band in turn undergoes a Mott transition. We observe that, within slave-spin mean field, the quasipar-

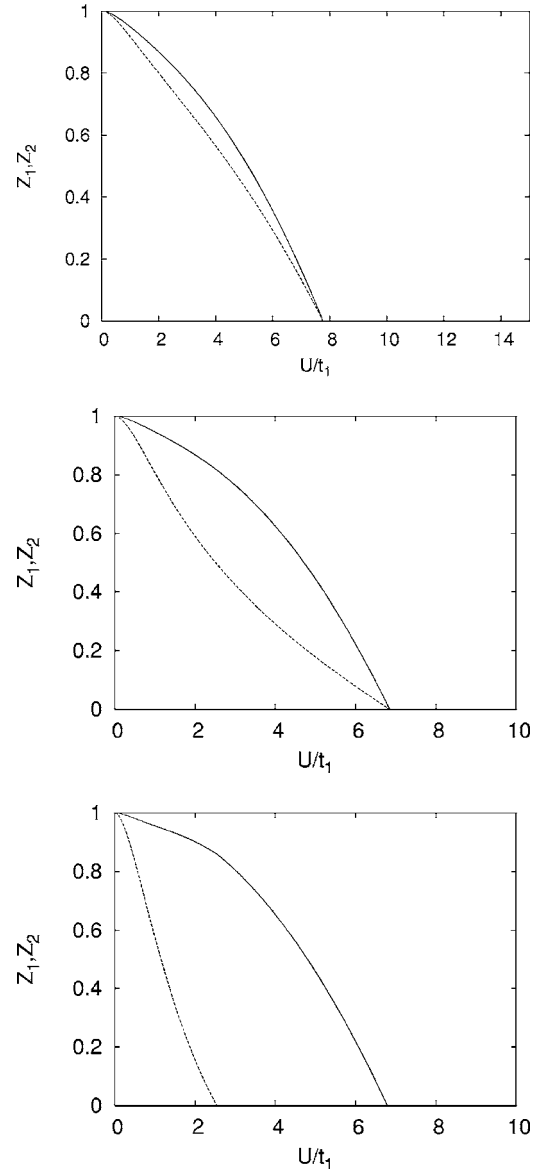


FIG. 6. Z_m at $J=0$ and $T=0$ for $t_2/t_1=0.5$ (top), 0.25 (middle), 0.15 (bottom).

ticle weight of the wider band in the orbital-selective Mott phase coincides with that of a single-band model. This is because the slave-spin mean field neglects charge fluctuations of the localized orbital, so that the physical behavior of the wide band becomes effectively that of a one-band model as soon as the narrow band becomes localized.

Our finding of an orbital-selective Mott transition at $J=0$ when t_2/t_1 is small enough, within slave-spin mean-field theory, raises two questions. First, is this finding an artifact of the slave-spin approximation or does it survive a full DMFT treatment (i.e., is it a genuine feature of the infinite-coordination model)? Second, does this invalidate the argument based on the symmetry of H_{int} ? The first question will be addressed in detail in Sec. V in which a DMFT study will be performed, using exact diagonalization and quantum Monte-Carlo techniques. We will show that, indeed, a transition does exist at $J=0$ when t_2/t_1 is small enough, but that the nature of the intermediate phase (OSMP) at low energy is

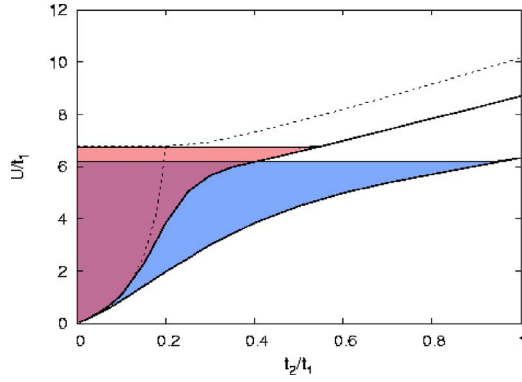


FIG. 7. (Color online) Widening of the OSMT zone with increasing J/U at $T=0$. Transition lines are shown for (from left to right) $J/U=0$ (dashed line), 0.01, 0.1.

a rather subtle issue. In order to address the second question, let us briefly recall the symmetry argument of Koga *et al.*⁹ The argument relies on the gap to charge-excitations in the insulating phase. When $J=0$, charge excitations mix the two orbitals because of the enhanced $SU(4)$ symmetry. Instead, for $J \neq 0$, the charge excitations of lowest energy are independent in each orbital sector. As a result, it is reasonable to expect (at least when the kinetic energy term is treated in a perturbative manner) that the system can sustain two different charge gaps when $J \neq 0$ while the gaps might coincide for $J=0$. We observe, however, that this argument applies to the instability of the large- U Mott phase (in which both bands are gapped) when U is reduced and suggests that, for $J=0$, the Mott gap closes at the same value of U for both bands when U/t_1 is reduced. It does not preclude, however, that a transition into an intermediate phase does exist, in which the “localized” band (with the narrower bandwidth) is not fully gapped. As we shall find below, there is indeed clear evidence from the DMFT results that the orbital-selective Mott phase at $J=0$ is *not a conventional Mott insulator* and that the narrow (“localized”) band does have spectral weight down to zero energy in this phase. Obviously, the slave-spin mean-field approach is too rudimentary to be able to capture these fine low-energy aspects, but it is remarkable that it does allow us to infer correctly that an intermediate phase is indeed present.

B. Dependence of OSMT on J

Having clarified the situation for $J=0$, we come back to the effect of a nonzero J , still within the slave-spin mean-field approximation. Figure 7 shows how the phase diagram as a function of the bandwidth ratio t_2/t_1 and of U/t_1 is modified for $J \neq 0$. One sees that a finite J enlarges the orbital-selective Mott phase and favors an OSMT. The critical ratio $(t_2/t_1)_c$ below which an OSMP exists increases significantly—e.g., $t_2/t_1 \approx 0.55$ for $J=0.01U$. With increasing J , $(t_2/t_1)_c$ tends towards 1. Hence a common Mott transition for both bands is recovered for all values of J only when $t_1=t_2$. For a given bandwidth ratio t_2/t_1 , the Mott transition is orbital selective for $J/U > (J/U)_c$. The dependence of this critical ratio upon t_2/t_1 (i.e., the location of the en-

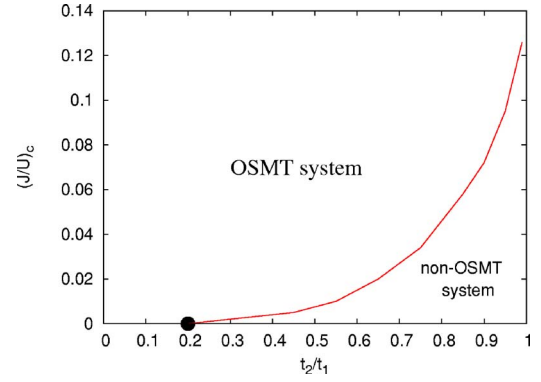


FIG. 8. (Color online) Dependence of the critical J/U above which the Mott transition becomes orbital selective on the ratio t_2/t_1 at $T=0$.

point of the OSMP phase) is displayed in Fig. 8. [It should be noted, however, that this critical ratio $(J/U)_c$ is underestimated by our simplified treatment of the pair-hopping and spin-flip terms.] Finally, we found that for finite J , the insulator-to-OSMP transition remains second order, while the metal-to-OSMP transition becomes first order.

C. Role of the spin-flip and pair-hopping terms in the Hund Hamiltonian

In order to clarify the role played by the different terms of the interaction (2), we have also studied the Hamiltonian in which the spin-flip and the (on-site) interorbital pair-hopping terms are dropped: namely,

$$H_{int} = U \sum_{im} \tilde{n}_{im\uparrow} \tilde{n}_{im\downarrow} + (U - 2J) \sum_{i\sigma} \tilde{n}_{i1\sigma} \tilde{n}_{i2\bar{\sigma}} + (U - 3J) \sum_{i\sigma} \tilde{n}_{i1\sigma} \tilde{n}_{i2\sigma}, \quad (25)$$

which is easily represented in terms of slave spins as

$$H_{int} = \frac{U'}{2} \sum_i \left(\sum_{m,\sigma} S_{im\sigma}^z \right)^2 + J \sum_{i,m} \left(\sum_{\sigma} S_{im\sigma}^z \right)^2 - \frac{J}{2} \sum_{i,\sigma} \left(\sum_m S_{im\sigma}^z \right)^2. \quad (26)$$

This study is also motivated by a comparison to quantum Monte Carlo treatments in which the spin-flip and pair-hopping terms are not easily treated. In Fig. 9 we display the slave-spin phase diagram found for $t_2/t_1=0.5$ at zero temperature. One sees that the OSMP shrinks dramatically (albeit the two transitions do not actually merge). This finding sheds light on the results by Liebsch in Refs. 7, 8, and 10. Because this study was based on quantum Monte Carlo calculations, hence neglecting the spin-flip and pair-hopping terms, it is natural that the orbital-selective phase can be found only in a very narrow range of parameter space. The key role of spin-flip and interorbital pair-hopping terms for the OSMT was actually pointed out in the recent work of Koga *et al.*¹¹

In Fig. 10, we display the region in $t_2/t_1, J/U$ parameter space where the Mott transition is found to be orbital selec-

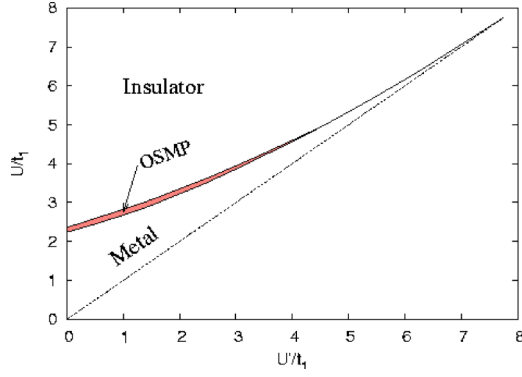


FIG. 9. (Color online) Phase diagram (U vs U') for $t_2/t_1=0.5$ at $T=0$ for a two-band Hubbard model without spin-flip and pairing terms in the interaction.

tive, analogously to Fig. 8. The critical ratio $(J/U)_c$ is found to be roughly exponential in t_2/t_1 . In contrast to the case of the full Hamiltonian (Fig. 8), we find that no OSMT exists when t_2/t_1 exceeds a critical bandwidth ratio $t_2/t_1 \approx 0.6$ for any J/U . (Note that the upper critical line at large J/U corresponds, however, to the unphysical case of an attractive Coulomb interaction due to $U-3J < 0$.)

Finally, we emphasize that the orbital-selective Mott phase, which exists only in a very narrow range of couplings for the simplified interaction (25) at $T=0$, is actually enlarged at finite temperature, as shown in Fig. 11.

V. DYNAMICAL MEAN-FIELD THEORY FOR $J=0$ AND THE NATURE OF THE OSMT PHASE

In this section, we study the two-band model with $J=0$ using dynamical mean-field theory. Our goal is to determine whether the transition into an OSMP found within the slave-spin approximation at small enough t_2/t_1 is indeed a robust feature and to shed light on the possible low-energy physics of this phase. Within DMFT, the lattice model is mapped

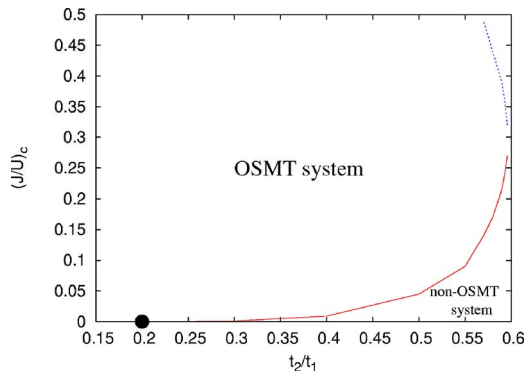


FIG. 10. (Color online) Critical J/U for the model without spin-flip and pair-hopping terms as a function of t_2/t_1 . At small ratios of the bandwidths, the system displays an OSMT above a critical J/U ratio which vanishes at $t_2/t_1=0.2$. In less anisotropic systems large Hund's couplings are needed to realize OSMP's, whereas beyond the critical bandwidth ratio of 0.6 no OSMT is possible within this model.

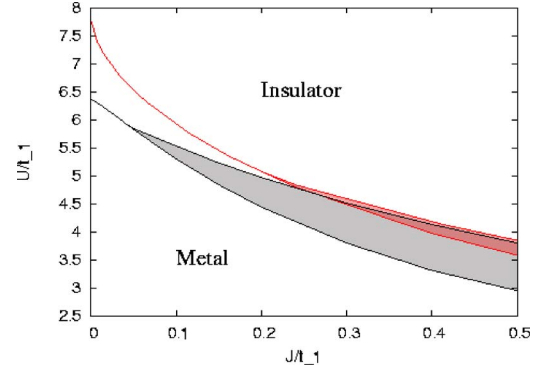


FIG. 11. (Color online) Same phase diagram as in Fig. 9 but in the U - J plane at $T=0$ and at $\beta t_1=40$.

onto a self-consistent two-orbital Anderson impurity model^{20,1} with effective action

$$-\int_0^\beta \int_0^\beta d\tau d\tau' \sum_{m\sigma} d_{m\sigma}^\dagger(\tau) \mathcal{G}_m^{-1}(\tau - \tau') d_{m\sigma}(\tau') + \frac{U}{2} \int_0^\beta d\tau (n_1 + n_2 - 2)^2. \quad (27)$$

The hybridizations to the effective conduction bath are self-consistently related to the local interacting Green's functions G_m through

$$\mathcal{G}_m(i\omega_n)^{-1} = i\omega_n - t_m^2 G_m(i\omega_n). \quad (28)$$

These equations are exact for an infinite-connectivity Bethe lattice [corresponding to a semicircular noninteracting density of states (DOS)]. Particle-hole symmetry with one electron per site in each band has been assumed. We focus here on the paramagnetic solutions only. The DMFT equations will be solved in the following using both an exact diagonalization (ED) and quantum Monte Carlo (QMC) technique.

A. Exact diagonalization study

Within the adaptative exact-diagonalization method,^{1,21} the effective conduction-electron bath is discretized using a finite number of orbitals, N_s . Hence, one considers the two-orbital Anderson impurity Hamiltonian:

$$H_{AIM} = \sum_{m\sigma} \sum_{l=1}^{N_s} \epsilon_{lm} a_{lm\sigma}^\dagger a_{lm\sigma} + \sum_{m\sigma} \sum_{l=1}^{N_s} V_{lm} (d_{m\sigma}^\dagger a_{lm\sigma} + \text{H.c.}) + \frac{U}{2} (\hat{n}_1 + \hat{n}_2 - 2)^2. \quad (29)$$

The operators $a_{lm\sigma}$, $a_{lm\sigma}^\dagger$ describe the discretized conduction bath degrees of freedom. The effective parameters $\{\epsilon_{lm}, V_{lm}\}$ have to be determined self-consistently, according to Eq. (28): namely,

$$\sum_{l=1}^{N_s} \frac{|V_{lm}|^2}{i\omega_n - \epsilon_{lm}} = t_m^2 G_m(i\omega_n). \quad (30)$$

The ED method becomes an asymptotically exact solver of the DMFT equations in the limit $N_s \rightarrow \infty$. In practice, how-

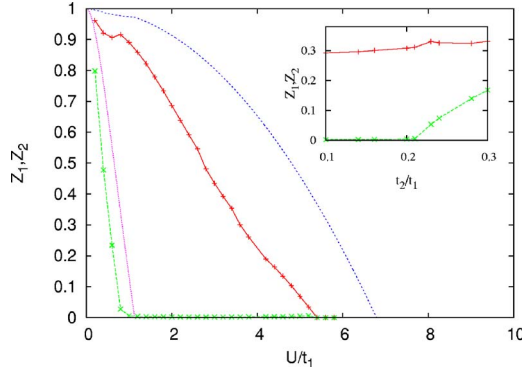


FIG. 12. (Color online) Quasiparticle residues at $J=0$ in DMFT (ED) for $t_2/t_1=0.1$ (symbols). For comparison, the slave-spin mean-field approximation is also displayed (solid line). Inset: same quantities as a function of t_2/t_1 at fixed $U/t_1=4.0$. (The kinks in Z_1 are associated with the criticality of Z_2 .)

ever, one can handle only a finite number of effective sites. For the case at hand, we used a $T=0$ Lanczos algorithm, with $N_s=5$ (i.e., 5 effective sites per orbital). The self-consistency (30) is implemented on a Matsubara grid corresponding to a (fictitious) inverse temperature β (taken to be in practice in the range 200–500, which ensures a good resolution on the low-energy physics). We monitor in particular the quasiparticle weights, approximated as $Z_m=[1-\text{Im}\Sigma_m(i\omega_0)/\omega_0]^{-1}$ [where $\omega_n=\pi/\beta(2n+1)$].

Our ED results for these quantities are displayed in Fig. 12 and compared to the slave-spin results, both as a function of U for fixed t_2/t_1 and as a function of t_2/t_1 for fixed U (inset). It is clear from this figure that, within the energy resolution which can be reached with $N_s=5$, an orbital-selective transition is indeed observed in the DMFT (ED) results when t_2/t_1 is smaller than a critical value (close to 0.25), in remarkable agreement with the slave-spin mean field. The quantitative value of the critical coupling U/t_1 for the localization of the wider band is overestimated, as usual in Gutzwiller-like schemes.

The phase diagram obtained with ED, as a function of t_1/t_2 and U/t_1 , is displayed in Fig. 13. Good qualitative agreement with the slave-spin mean field is found (Fig. 5). We also studied the hysteresis properties by performing runs for increasing and decreasing values of U/t_1 . This results in two almost parallel transition lines in Fig. 13, one corresponding to the disappearance of the metallic solution (obtained from a series of runs for increasing U), the other corresponding to the loss of the insulating nature of the wide band (from a series of runs for decreasing U). In the region between these two lines, coexistence of two types of DMFT solutions is found: for small t_2/t_1 , one of the solutions is orbital selective Mott and the other is fully insulating, while for larger t_2/t_1 , one of the solutions is metallic and the other fully insulating. The actual thermodynamic transition is given by the crossing of the free energies of the two solutions. In contrast, no hysteresis has been found at the transition between the OSMP and metallic phases. This suggests that the transition from the metallic to the OSMP phase is of a very different nature than the Mott transition of the wider band. If only the gap closure is monitored, then only one

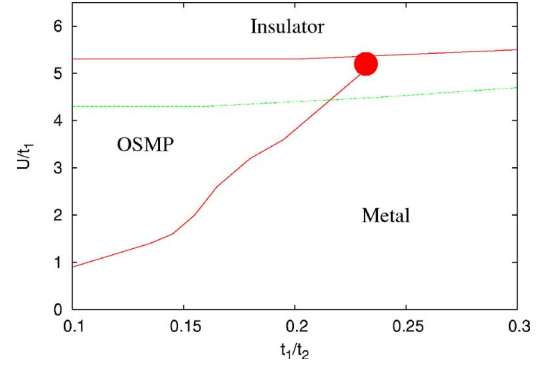


FIG. 13. (Color online) Phase diagram at $J=0$ and $T=0$ in ED DMFT. The dashed line marks the disappearance of the Mott gap (downward runs). For U values around 5 there is coexistence between an OSMP and—depending on the bandwidth ratio—an insulating or metallic phase.

transition is found at $J=0$, in agreement with the symmetry argument of Ref. 9. As we shall demonstrate below, there is indeed strong evidence that the orbital-selective Mott phase at $J=0$ does not display a sharp gap in either orbitals.

B. Low-energy nature of the orbital-selective Mott phase at $J=0$, from ED and QMC techniques

In order to understand better the nature of the orbital-selective phase found at $J=0$, we take a closer look at the local Green's function for each orbital in each phase. In order to do this, we also solved the DMFT equations using the quantum Monte Carlo algorithm of Hirsch and Fye.²² The ED and QMC methods are quite complementary. The former applies at $T=0$ but suffers from a limited energy resolution due to the small value of N_s , while the latter is limited to finite temperature but can be made very precise by increasing the number of time slices and the number of Monte Carlo sweeps (we used 128 slices in imaginary time and up to 5×10^5 Monte Carlo sweeps in practice). Also, using the QMC technique allows for a reconstruction of the spectral functions using a numerical analytic continuation based on the maximum entropy algorithm.

In Fig. 14, we display the ED results for the local Green's functions on the Matsubara axis, for a small bandwidth ratio t_2/t_1 and three different values of U corresponding to the insulating, metallic, and orbital-selective Mott phases. In the particle-hole-symmetric case, the Green's functions are purely imaginary on the Matsubara axis and related to the spectral function $A_m(\epsilon)$ of each orbital by

$$\text{Im} G_m(i\omega) = -2\omega \int_0^{+\infty} d\epsilon \frac{A_m(\epsilon)}{\omega^2 + \epsilon^2}. \quad (31)$$

When the spectral function $A_m(\epsilon)$ has a gap, the integral in the right-hand side of Eq. (31) has no singularity in the $\omega \rightarrow 0$ limit, and hence $\text{Im} G_m(i\omega) \propto \omega$ at low frequency. Furthermore, $\text{Im} G_m(i\omega)$ has a minimum for ω of order $\Delta_m/2$, with Δ_m the gap in the m th orbital (as can be seen by replacing $A_m(\epsilon)$ by the simplified form $1/2[\delta(\epsilon-\Delta_m/2)+\delta(\epsilon+\Delta_m/2)]$, yielding $\text{Im} G_m(i\omega) \approx -2\omega/(\omega^2+\Delta_m^2/4)$). This is

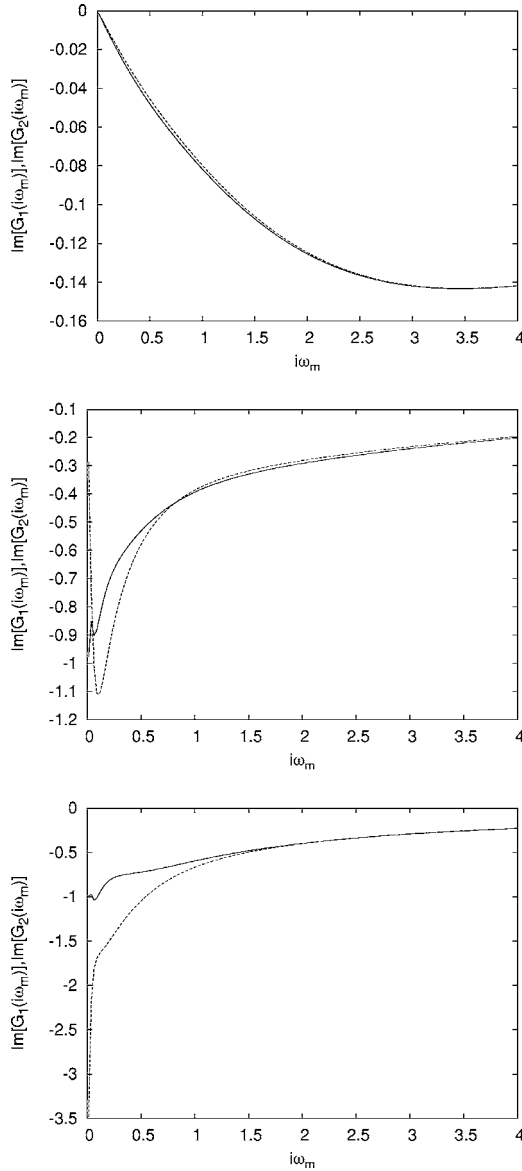


FIG. 14. Imaginary part of the Green functions of the two bands at low energy for $t_2/t_1=0.16$. Upper panel: $U/t_1=7.0$, both bands are insulating. Central panel: $U/t_1=4.0$, orbital-selective Mott phase. Lower panel: $U/t_1=2.0$, both bands metallic. The dashed curves correspond to the orbital with narrower bandwidth. All energy scales are in units of t_1 .

fully consistent with the ED results in the upper panel of Fig. 14, corresponding to a large value of $U/t_1=7$, with both orbitals insulating and having a gap of order U .

In the lower panel of Fig. 14, ED results are displayed for $U/t_1=2$, when both orbitals are metallic. In this case, the low-frequency limit of Eq. (31) yields $\text{Im} G_m(i\omega \rightarrow 0) = -\pi A_m(0)$. This is consistent with the numerical results, which also show that the Luttinger theorem is obeyed for both bands: $\pi A_m(0) = 1/t_m$.

The central panel of Fig. 14 displays the ED results for an intermediate coupling, corresponding to the orbital-selective phase. One sees that the wider band has metallic behavior, with $A_1(\omega)$ still reaching the Luttinger value at $\omega=0$. In contrast, $\text{Im} G_2(i\omega)$ appears to vanish as $\omega \rightarrow 0$, within the en-

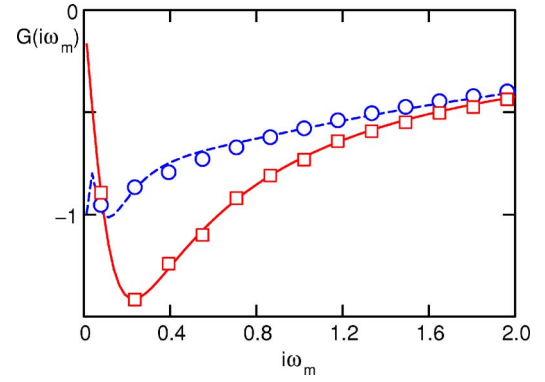


FIG. 15. (Color online) Imaginary parts of the Green's functions in Matsubara space for $t_2/t_1=0.1$, $U/t_1=1.6$. Solid and dashed lines represent the exact diagonalization results for the wide and narrow bands, respectively. Circles and squares represent QMC data for the same quantities at $\beta t_1=40$.

ergy resolution of ED. However, in striking contrast to the upper panel (insulating phase), the minimum in $\text{Im} G_2(i\omega)$ is at a *very-low-frequency scale* which is obviously not given by U . This strongly suggests that $A_2(\omega)$ displays low-energy peaks very close to $\omega=0$ and may even have spectral weight down to arbitrary low frequency.

Figure 15 compares the ED and QMC results for $\text{Im} G_{1,2}(i\omega)$ in the strongly anisotropic case $t_2/t_1=0.1$ for a relatively small Coulomb interaction $U/t_1=1.6$, easier to study with the QMC technique. These parameters also correspond to the orbital-selective phase (Fig. 13). Very good agreement between the two methods is found, confirming the above analysis (and confirming also the Luttinger value for the wider band with greater accuracy than in ED). The corresponding spectral functions obtained by the maximum-entropy method are displayed on Fig. 16. The spectral function of the broader band is only slightly modified as compared to the noninteracting DOS. Small shoulders are visible, at the position of the lower and upper Hubbard bands, the Luttinger theorem is obeyed, and some of the spectral weight is transferred to higher energies as expected. The narrow band, however, is obviously in a strong-coupling

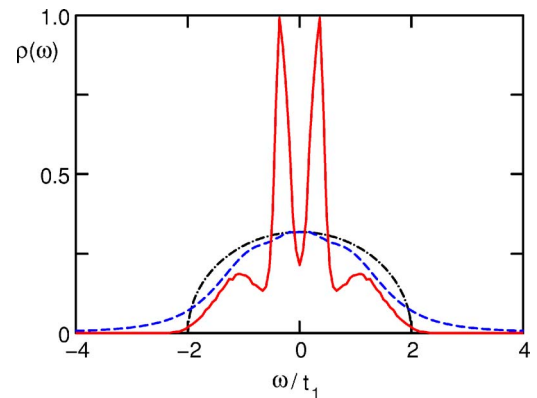


FIG. 16. (Color online) Spectral function for $t_2/t_1=0.1$, $U/t_1=1.6$ at $\beta t_1=40$ in QMC DMFT. The solid and dashed red lines denote the narrow and wide bands, respectively. The DOS of the noninteracting system (wide band only) is given for comparison.

regime, with well-marked upper and lower Hubbard bands. The most striking features, however, are the two narrow peaks at low frequency, which can be interpreted either as a split quasiparticle resonance or as the sign of a *pseudogap* (partially filled by thermal excitations since the QMC calculation is for $T/t_1=1/40$).

Hence, the general conclusion of this analysis is that the orbital-selective phase found for $J=0$ at small enough t_2/t_1 is not a conventional Mott phase in which the (“localized”) orbital with narrower bandwidth would display a sharp gap. Instead, two narrow peaks exist near $\omega=0$ and finite spectral weight is found down to low energy. Our numerical data are consistent with a pseudogap behavior, but a precise characterization of the low-energy nature of the phase will require further effort, using highly precise techniques at low energy such as the numerical renormalization group. This is left for future work. Such a study should also clarify in which precise sense the narrower band is “localized” in this phase and whether the orbital-selective transition is a true phase transition or rather a sharp crossover.

VI. INSTABILITY OF THE ORBITAL-SELECTIVE MOTT PHASE UPON INTERBAND HYBRIDIZATION

To what extent an orbital-selective Mott phase may occur in practice depends on its stability with respect to perturbations. This is an important issue in view of the fact that the Hamiltonian considered in this paper has a rather high degree of symmetry. In this last section, we consider the effect of an hybridization between the two orbitals (also recently considered in Ref. 25)—i.e., of a local nondiagonal term

$$H_{hyb} = V \sum_{i\sigma} (d_{i1\sigma}^\dagger d_{i2\sigma} + d_{i2\sigma}^\dagger d_{i1\sigma}). \quad (32)$$

We note that this term could be eliminated by diagonalizing the noninteracting Hamiltonian. However, in the new basis, the interaction terms will be modified: terms will be generated which will have the same physical effect than a hybridization (and will involve nonlocal contributions in general). Indeed, as emphasized in Ref. 23, the existence of an OSMT is a *basis-independent* issue. In a general two-band model, a Mott transition is signaled, when approached from the metallic side, by a low-frequency singularity in $\omega \hat{I} - \hat{\Sigma}(\omega) = \hat{Z}^{-1} \omega + \dots$, where $\hat{\Sigma}$ and \hat{Z} are the self-energy and quasiparticle-weight matrices, respectively. An OSMT is characterized by \hat{Z} having one zero eigenvalue while the other one remains finite. Being associated with the rank of the \hat{Z} matrix, it is a basis-independent notion. Our choice of basis is such that the interaction terms have the form specified above.

A. Physical considerations

Some statements about the effect of a finite hybridization can be made on general physical grounds (focusing for simplicity on the $J=0$ case). First, for small values of U when both orbitals are itinerant, it is obvious that a hybridization will not change qualitatively the low-energy nature of the

metallic phase. Also, at very large U , when both orbitals are localized and a gap exists in both orbital sectors, we expect the presence of a gap to be a robust feature which persists in the presence of V . However, it is also clear that introducing V into this gapped insulator allows the local moments formed in the Mott insulating state at $V=0$ to screen each other. This occurs through the formation of on-site bonding and antibonding “molecular” levels mixing the two orbitals. As a result, the local-moment Mott insulator is expected to be replaced by a Mott insulator in which *local singlets* are formed on each site. Note that this is true even at finite J , but only as long as $J < V$. When $J > V$, a triplet groundstate ($S=1, S^z=0$) is rather expected based on the analogue crossing of groundstates that is found in the atomic limit. The intermediate- U regime, in which the system is in the OSMP at $V=0$, is more delicate. Because orbital 1 is itinerant, a Kondo screening process can take place, which will screen the local moment (formed by orbital 2 when $V=0$). The resulting state can *a priori* be either a heavy-fermion metallic state involving quasiparticles with a large effective mass or (because we are considering the half-filled case) a Kondo insulating state in which a gap is formed in the low-energy quasiparticle spectrum. Below, we study this question using the slave-spin approach and find that both phases can be obtained, depending on the value of U and V . A larger V favors the opening of a gap, as expected. Using a general low-frequency analysis, we also demonstrate that, for small values of V , the heavy-fermion metallic state, and not the Kondo insulating phase, is induced. We note, finally, that both the Kondo-insulating phase and the phase obtained at large U when $J=0$, in which on-site local moments in different orbitals screen each other have a singlet ground-state. It is therefore not obvious *a priori* whether these two phases are continuously connected,²⁵ as found in Ref. 26 and 27 for a related (but different) model, or whether a phase transition between them can exist. We return to this point at the end of this section.

In any event, these physical arguments imply that the orbital-selective Mott phase is unstable with respect to the introduction of a nonzero hybridization at zero-temperature. Of course, for temperatures above the Kondo scale, the physics of the OSMP can be recovered. This is an important point in view of the possible experimental relevance of the OSMP.

B. Slave-spin mean-field study

We now turn to a more quantitative study of the effect of a finite hybridization (32) using the slave-spin mean-field approximation. Our aim is not to establish a full phase diagram for all values of the parameters U , J , and V , but rather to investigate whether this approach does support the physical expectations discussed above. A more extensive investigation will be presented in a future publication.

In Fig. 17, we display the quasiparticle residues Z_1 (for the broad band) and Z_2 (for the narrow band) as a function of U and for increasing values of the hybridization V . It is seen that, starting from the OSMP in which $Z_1 \neq 0$ and $Z_2=0$ for $V=0$, one obtains either a phase in which both Z_1 and Z_2 are nonzero (i.e., Kondo screening takes place) or an insulating

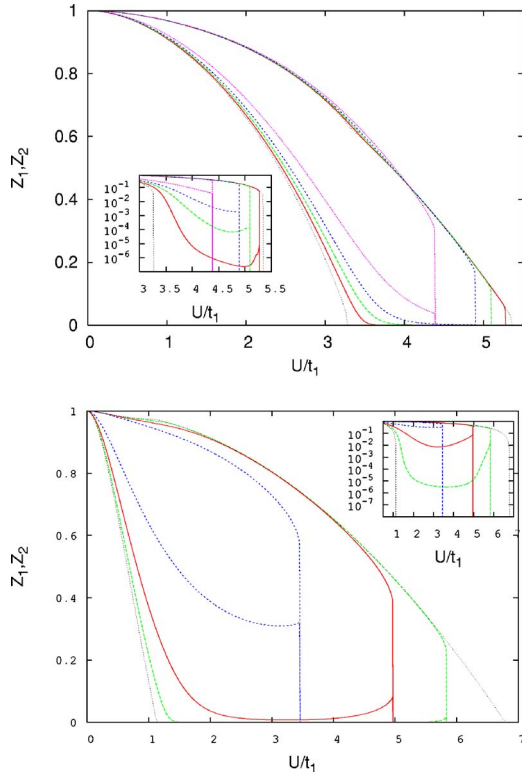


FIG. 17. (Color online) Quasiparticle residues Z_1 and Z_2 within slave-spin MFT for finite V . Top: $t_2/t_1=0.5$, $J=0.25U$ for (from right to left in the upper manifold, wide band; from left to right in the lower manifold, narrow band): $V=0$ (OSMT system), $V/t_1=0.1, 0.15, 0.2, 0.3$. Bottom: $t_2/t_1=0.1$, $J=0$ for (from right to left in the upper manifold, wide band; from left to right in the lower manifold, narrow band) $V=0$ (OSMT system), $V/t_1=0.05, 0.1, 0.2$. Insets show the same graph in logarithmic scale.

phase in which $Z_1=Z_2=0$. This demonstrates that the hybridization is indeed a singular perturbation on both the $J=0$ and finite- J orbital-selective Mott phases, in agreement with the physical arguments above.

In order to check whether the Kondo-screened phase is a (heavy-fermion) metal or whether it is gapped (Kondo insulator), we have plotted in Fig. 18 the band gap of the auxiliary quasiparticles found within slave-spin mean-field theory (the plot is for $J=0$, the $J \neq 0$ case being similar). Note that due to the factorization of the Green's function,

$$\langle d(\tau)_{m\sigma} d_{m\sigma}^\dagger(0) \rangle = 4 \langle S^x(0)_{m\sigma} S^x(\tau)_{m\sigma} \rangle \langle f_{m\sigma}(\tau) f_{m\sigma}^\dagger(0) \rangle, \quad (33)$$

the physical gap in the insulating phase will be of the order U . For small and intermediate values of V , the phase with $Z_1 \neq 0$ and $Z_2 \neq 0$ is metallic (gapless) (see Fig. 18). The orbital-selective Mott phase is replaced by a heavy-fermion regime, as shown in Fig. 17, in which the orbital with narrower bandwidth acquires a very large effective mass (corresponding to a very low quasiparticle coherence scale Z_2). This is also in qualitative agreement with our recent study of the periodic Anderson model with direct f -electron hopping.²³ Only beyond a critical value of V is a gapped

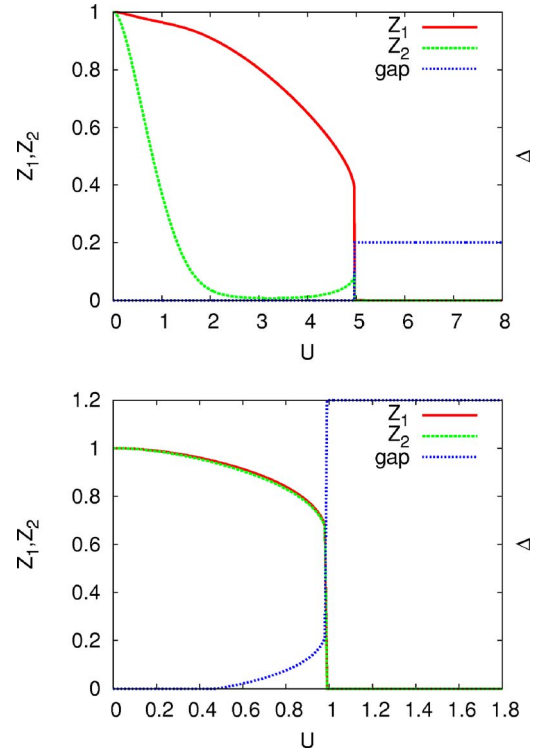


FIG. 18. (Color online) Gap amplitude of the auxiliary fermions (see text) and quasiparticle residues within slave-spin MFT for two values of V . Top: $t_2/t_1=0.1$, $J=0$ for $V/t_1=0.1$ (upper panel) and $V/t_1=0.6$ (lower panel). The corresponding critical V for the non-interacting system is $\sqrt{D_1 D_2} \approx 0.63$ in this case.

Kondo insulator found. As discussed below, this can in fact be proven generally, beyond the mean-field approximation used here.

At small to intermediate values of V , the two Mott transitions associated with the OSMP at $V=0$ are therefore replaced by a single nonselective transition from a (heavy-fermion) metal to an insulator as U is increased. Within the slave-spin mean field, this unique metal-to-insulator transition is found to be first order and to occur at a critical value of U which lies in between the critical interactions of the metal-OSMP and OSMP-insulator transitions.

For larger values of V , the OSMP phase is replaced by a Kondo-insulating phase with $Z_1, Z_2 \neq 0$ but a finite quasiparticle band gap (lower plot in Fig. 17). Within slave-spin mean-field theory, a phase transition takes place, as U is increased, towards another insulating phase with $Z_1=Z_2=0$ (corresponding to the fact that the Kondo effect does not take place when V is turned on starting from a Mott phase for both orbitals with a large gap). As pointed out above, however, the large- U insulating phase at $J < V$ also has a singlet ground state, however, due to interorbital screening. Whether this phase transition is an artifact of the slave-spin mean field or whether it is indeed present in a more accurate DMFT treatment is a question to which we shall return below.

C. General low-frequency analysis

In order to understand better the nature of both the metallic and insulating phases to which the OSMP is driven for

$V \neq 0$, we perform here a low-energy analysis in terms of a renormalized quasiparticle band structure (see also Ref. 27). We focus on the case in which the Kondo effect does take place as V is turned on, resulting in both quasiparticle residues being finite. We thus keep the following terms in the low-frequency expansion of the self-energy:

$$\begin{aligned}\bar{\Sigma}_{11}(\omega) &= \omega(1 - 1/Z_1) + \dots, \\ \bar{\Sigma}_{22}(\omega) &= \omega(1 - 1/Z_2) + \dots, \\ \Sigma_{12}(\omega) &= \Sigma_{12}(0) + \dots.\end{aligned}\quad (34)$$

The low-energy quasiparticle band structure is then given by

$$[\omega - Z_1 \epsilon_1(\mathbf{k})][\omega - Z_2 \epsilon_2(\mathbf{k})] - Z_1 Z_2 [V + \Sigma_{12}(0)]^2 = 0. \quad (35)$$

From this expression, it is easily seen that a gap is present whenever

$$V_{\text{eff}} > \sqrt{D_{1\text{eff}} D_{2\text{eff}}}. \quad (36)$$

In this expression, V_{eff} is the effective hybridization between low-energy quasiparticles and $D_{1\text{eff}}, D_{2\text{eff}}$ the renormalized quasiparticle half-bandwidths given by

$$V_{\text{eff}} = \sqrt{Z_1 Z_2} [V + \Sigma_{12}(0)], \quad D_{1\text{eff}} = Z_1 D_1, \quad D_{2\text{eff}} = Z_2 D_2. \quad (37)$$

Remarkably, Z_1 and Z_2 drop out from (36), and the condition for a quasiparticle band gap therefore reads

$$V + \Sigma_{12}(0) > \sqrt{D_1 D_2}. \quad (38)$$

If this condition is satisfied (and $Z_1, Z_2 \neq 0$), one has a Kondo insulator phase, with a quasiparticle band gap given by

$$\Delta_g = \sqrt{(D_{1\text{eff}} - D_{2\text{eff}})^2 + 4V_{\text{eff}}^2} - (D_{1\text{eff}} + D_{2\text{eff}}). \quad (39)$$

In the opposite case, a heavy-fermion (gapless) metallic phase is formed.

From (38), it is seen that it is the off-diagonal component of the self-energy (induced by V) which plays the key role in deciding whether a gap opens or not. From the same equation, it is also clear that a *band gap cannot open for arbitrary small V* . Indeed, at small V , Σ_{12} grows at most proportionally to V , and hence the left-hand side of (38) is small, while the right-hand side (RHS) is finite (note that the RHS involves the *bare* bandwidths). Hence, a critical value of V is required to open a band gap and enter the Kondo insulating phase, starting from the OSMP. Note that this analysis is general and relies only on Fermi-liquid considerations, independently of the specific method used to solve the model. Note also that the situation is very different when one of the bare bands is dispersionless ($D_2=0$), as is the case of the periodic Anderson models considered in Refs. 26 and 27. In this case, it is clear from (38) that an arbitrarily small V induces the Kondo-insulating state. The formation of a heavy-fermion metallic state induced by a nonzero hybridization in a generalized periodic Anderson model with $D_2 \neq 0$ (direct f -electron hopping) was also investigated in our recent work.²³

The slave-spin mean-field results presented above can be placed in the context of this general low-frequency analysis. Within this approach, one has

$$Z_1 = 4\langle S_1^x \rangle^2, \quad Z_2 = 4\langle S_2^x \rangle^2, \quad V_{\text{eff}} = 4\langle S_1^x S_2^x \rangle V. \quad (40)$$

It is important to realize that this approach does provide an off-diagonal component of the physical electron self-energy, which, using Eqs. (37), is given by

$$\frac{\Sigma_{12}(0)}{V} = \frac{\langle S_1^x S_2^x \rangle - \langle S_1^x \rangle \langle S_2^x \rangle}{\langle S_1^x \rangle \langle S_2^x \rangle}. \quad (41)$$

Note that in more conventional slave-boson approaches, the physical electron operators are related to the quasiparticles by a slave-boson condensation amplitude which is a c number ($d_m^\dagger = \sqrt{Z_m} f_m^\dagger$). As a result, $V_{\text{eff}} = \sqrt{Z_1 Z_2} V$, and no off-diagonal component of the self-energy is present. In such slave-boson approaches, the condition for the presence of a quasiparticle band gap is therefore entirely unrenormalized by interactions and reads $V/\sqrt{D_1 D_2} > 1$. This is an oversimplification which is not present in the slave-spin approach. There, the criterion for the opening of a gap reads

$$\frac{V}{\sqrt{D_1 D_2}} > \frac{\langle S_1^x \rangle \langle S_2^x \rangle}{\langle S_1^x S_2^x \rangle}. \quad (42)$$

However, despite the renormalization of the hybridization by the off-diagonal self-energy, we find that in practice this criterion is very close to the noninteracting one, which gives a reasonable approximation of the critical hybridization necessary to open a band gap.

Finally, we comment on the phase transitions between the different phases induced by a nonzero hybridization. At small V , it is clear that there must exist a phase transition between the metallic (gapless) heavy-fermion phase and the insulating (gapped) phase, as U is increased (as indeed seen in Fig. 18, top panel). The situation is less clear at larger V . There, if $J > V$, an actual transition is expected as U is increased, owing to the fact that a singlet groundstate is replaced by a triplet one, as soon as the system becomes insulating. When $V > J$ instead, we always expect an insulator with a singlet ground state. However, the mechanism behind this singlet formation is rather different at smaller and larger values of U . In the former case, Kondo screening dominates and the singlet is formed by screening the local moment in orbital 2 by the electrons in orbital 1. At larger U , the Kondo coupling is smaller, and it is the formation of an interorbital molecular bonding level (due to V) which is responsible for the singlet formation. Within slave-spin mean-field theory, we find a phase transition between these two kinds of insulator as U is increased, the latter one being signaled by $Z_1 = Z_2 = 0$ (Fig. 18, bottom panel). However, it is not clear whether this phase transition is a real feature or an artifact of the slave-spin approximation. In Ref. 25, Koga *et al.* recently suggested that these two phases should be adiabatically connected, as found also in the study of the periodic Anderson model with correlated conduction electrons^{26,27} (note, however, that the present model is different, in that both bands have a dispersion and that an interorbital interaction is present). The problem is qualitatively similar (but not

equivalent, because of the interorbital interaction) to the two-impurity Kondo problem,²⁸ in which the interimpurity singlet (RKKY) fixed points and the Kondo singlet fixed points are in general adiabatically connected (except in the special case of particle-hole symmetry, where a phase transition does occur). Note that it is well known²⁹ that for this latter model, slave-boson approximations do lead to spurious first-order transitions. A full answer to this question is beyond the scope of this paper and is left for a future investigation, together with a complete phase diagram as a function of interaction strength and hybridization.

VII. CONCLUSION

In this article, we have studied whether the Mott transition of a half-filled, two-orbital Hubbard model with unequal bandwidths occurs simultaneously for both bands or whether it is a two-stage process in which the orbital with narrower bandwidth localizes first (giving rise to an intermediate “orbital-selective” Mott phase). In order to study this question, we have used two techniques. The first is a mean-field theory based on a new representation of fermion operators in terms of slave quantum spins. This method is similar in spirit to the Gutzwiller approximation, and the slave-spin representation has a rather wide range of applicability to multiorbital models. The second method is dynamical mean-field theory, using exact diagonalization and quantum Monte Carlo solvers.

The results of the slave-spin mean field confirms several aspects of previous studies,^{9,11} and, in particular, the possibility of an orbital-selective Mott transition. However, some of the conclusions differ from those of previous work. Specifically, the slave-spin approximation suggests that a critical value of the bandwidth ratio $(t_2/t_1)_c$ exists, such that the Mott transition is orbital selective for an arbitrary value of the Coulomb exchange (Hund coupling) J when $t_2/t_1 < (t_2/t_1)_c$. When $t_2/t_1 > (t_2/t_1)_c$, J has to be larger than a finite threshold for an OSMT to take place. This suggests that the existence of an OSMT is not simply related to the symmetry of the interaction term only. In particular, an intermediate phase is found for $J=0$ at small t_2/t_1 .

We have studied whether DMFT confirms these findings and found that the main qualitative conclusions on the existence of the orbital-selective phase are indeed the same, but that the nature of the intermediate phase at $J=0$ is a rather subtle issue. Indeed, the narrow band does not have the properties of a gapped Mott insulator in this phase and displays

finite spectral weight down to arbitrary low energy. This is, for example, consistent with a pseudogap behavior but requires further studies to be fully settled (using, e.g., low-energy techniques such as the numerical renormalization group).

We note also that our study emphasizes the key role of the exchange and (on-site) interorbital pair hopping terms in the Coulomb Hamiltonian in stabilizing the orbital-selective phase, in agreement with Koga *et al.*¹¹

Finally, we found that the orbital-selective Mott phase is generically unstable with respect to an interorbital hybridization V . In the presence of such a term, two possible phases are obtained, depending on the strength of U and V . Either the narrow orbital acquires a large (but finite) effective mass, corresponding to a heavy-fermion metallic state. Or the system is an insulator with a gap. This insulator differs from the Mott insulator at $V=0$ since it has a singlet ground state. This is due to screening processes, involving both Kondo exchange and the formation of an on-site molecular (bonding) level. Whether one has in fact two different insulating phases separated by a phase transition (each phase being dominated by one of these screening processes)—as obtained by slave-spin mean-field theory—or whether one has a simple crossover²⁵ is an open question which deserves further study.

Of course, at intermediate temperature (above the quasiparticle coherence scale of the narrower band, but below that of the wider band), a physics similar to the orbital-selective Mott phase can be recovered even in the presence of a finite hybridization. This orbital-selective heavy-fermion state might be relevant to the physics of $\text{Ca}_{2-x}\text{Sr}_x\text{RuO}_4$. This is indeed supported by the recent angular magnetoresistance oscillations experiments of Balicas *et al.*²⁴

Note added. During the completion of this paper, we learned of the work³¹ by M. Ferrero, F. Becca, M. Fabrizio, and M. Capone, reaching similar conclusions.

ACKNOWLEDGMENTS

We are grateful to F. Becca, M. Fabrizio, and M. Capone for discussions. A.G. acknowledges discussions with S. Florens and N. Dupuis on the slave-spin representation at an early stage of this work. We are grateful to A. Lichtenstein for help with ED calculations in the multiorbital context. We also thank A. Koga, N. Kawakami, G. Kotliar, T.M. Rice, and M. Sigrist for useful discussions. This research was supported by CNRS and Ecole Polytechnique and by a grant of supercomputing time at IDRIS Orsay (Project No. 051393).

¹A. Georges, G. Kotliar, W. Krauth, and M. J. Rozenberg, *Rev. Mod. Phys.* **68**, 13 (1996).

²A. Georges, in *Lectures on the Physics of Highly Correlated Electron Systems VIII*, edited by A. Avella and F. Mancini (AIP, Melville, NY, 2004).

³G. Kotliar and D. Vollhardt, *Phys. Today* **57** (3), 53 (2004).

⁴A. Georges, S. Florens, and T. A. Costi, *J. Phys. IV* **114**, 165

(2004).

⁵V. Anisimov, I. Nekrasov, D. Kondakov, T. Rice, and M. Sigrist, *Eur. Phys. J. B* **25**, 191 (2002).

⁶Z. Fang, N. Nagaosa, and K. Terakura, *Phys. Rev. B* **69**, 045116 (2004).

⁷A. Liebsch, *Europhys. Lett.* **63**, 97 (2003).

⁸A. Liebsch, *Phys. Rev. B* **70**, 165103 (2004).

- ⁹A. Koga, N. Kawakami, T. M. Rice, and M. Sigrist, Phys. Rev. Lett. **92**, 216402 (2004).
- ¹⁰A. Liebsch, Phys. Rev. Lett. **91**, 226401 (2003).
- ¹¹A. Koga, N. Kawakami, T. Rice, and M. Sigrist, cond-mat/0406457 (unpublished).
- ¹²C. Castellani, C. R. Natoli, and J. Ranninger, Phys. Rev. B **18**, 4945 (1978).
- ¹³R. Frésard and G. Kotliar, Phys. Rev. B **56**, 12909 (1997).
- ¹⁴G. Kotliar and A. E. Ruckenstein, Phys. Rev. Lett. **57**, 1362 (1986).
- ¹⁵J. Bünenmann, F. Gebhard, and R. Thul, Phys. Rev. B **67**, 075103 (2003).
- ¹⁶S. Florens and A. Georges, Phys. Rev. B **66**, 165111 (2002).
- ¹⁷S. Florens and A. Georges, Phys. Rev. B **70**, 035114 (2004).
- ¹⁸S. Florens, A. Georges, G. Kotliar, and O. Parcollet, Phys. Rev. B **66**, 205102 (2002).
- ¹⁹S. Florens, P. San José, F. Guinea, and A. Georges, Phys. Rev. B **68**, 245311 (2003).
- ²⁰A. Georges and G. Kotliar, Phys. Rev. B **45**, 6479 (1992).
- ²¹M. Caffarel and W. Krauth, Phys. Rev. Lett. **72**, 1545 (1994).
- ²²J. E. Hirsch and R. M. Fye, Phys. Rev. Lett. **25**, 2521 (1986).
- ²³L. de' Medici, A. Georges, G. Kotliar, and S. Biermann, Phys. Rev. Lett. **95**, 066402 (2005).
- ²⁴L. Balicas *et al.*, cond-mat/0507457 (unpublished).
- ²⁵A. Koga, N. Kawakami, T. M. Rice, and M. Sigrist, Phys. Rev. B **72**, 045128 (2005).
- ²⁶T. Schork and S. Blawid, Phys. Rev. B **56**, 6559 (1997).
- ²⁷R. Sato *et al.*, J. Phys. Soc. Jpn. **73**, 1864 (2004).
- ²⁸B. A. Jones, C. M. Varma, and J. W. Wilkins, Phys. Rev. Lett. **61**, 125 (1988); B. A. Jones and C. M. Varma, Phys. Rev. B **40**, 324 (1989); I. Affleck and A. W. W. Ludwig, Phys. Rev. Lett. **68**, 1046 (1992); I. Affleck, A. W. W. Ludwig, and B. A. Jones, Phys. Rev. B **52**, 9528 (1995).
- ²⁹B. A. Jones, B. G. Kotliar, and A. J. Millis, Phys. Rev. B **39**, R3415 (1989).
- ³⁰Although the particle-hole symmetry of the present model gives rise to simplifications—e.g., on the implementation of the constraints ($\lambda_{im\sigma}=0$)—we present here the general procedure.
- ³¹M. Ferrero, F. Becca, M. Fabrizio, and M. Capone, Phys. Rev. B (to be published).